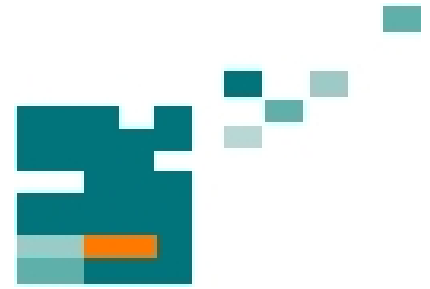


**54. IWK**  
Internationales Wissenschaftliches Kolloquium  
International Scientific Colloquium



**Information Technology and Electrical  
Engineering - Devices and Systems, Materials  
and Technologies for the Future**



Faculty of Electrical Engineering and  
Information Technology

Startseite / Index:

<http://www.db-thueringen.de/servlets/DocumentServlet?id=14089>

## Impressum

Herausgeber: Der Rektor der Technischen Universität Ilmenau  
Univ.-Prof. Dr. rer. nat. habil. Dr. h. c. Prof. h. c.  
Peter Scharff

Redaktion: Referat Marketing  
Andrea Schneider

Fakultät für Elektrotechnik und Informationstechnik  
Univ.-Prof. Dr.-Ing. Frank Berger

Redaktionsschluss: 17. August 2009

Technische Realisierung (USB-Flash-Ausgabe):  
Institut für Medientechnik an der TU Ilmenau  
Dipl.-Ing. Christian Weigel  
Dipl.-Ing. Helge Drumm

Technische Realisierung (Online-Ausgabe):  
Universitätsbibliothek Ilmenau  
[ilmedia](#)  
Postfach 10 05 65  
98684 Ilmenau

Verlag:  Verlag ISLE, Betriebsstätte des ISLE e.V.  
Werner-von-Siemens-Str. 16  
98693 Ilmenau

© Technische Universität Ilmenau (Thür.) 2009

Diese Publikationen und alle in ihr enthaltenen Beiträge und Abbildungen sind urheberrechtlich geschützt.

ISBN (USB-Flash-Ausgabe): 978-3-938843-45-1  
ISBN (Druckausgabe der Kurzfassungen): 978-3-938843-44-4

Startseite / Index:  
<http://www.db-thueringen.de/servlets/DocumentServlet?id=14089>

# MODULATION AND CODING ASPECTS FOR HOME GIGABIT ACCESS (OMEGA) USING WIRELESS INFRARED

*Liane Grobe, Jianhui Li, Mike Wolf and Martin Haardt*

Communications Research Laboratory  
Ilmenau University of Technology  
PO Box 100565 D-98684 Ilmenau, Germany  
Email: {Liane.Grobe, Jianhui.Li, Mike.Wolf, Martin.Haardt}@tu-ilmenau.de

## ABSTRACT

In this paper, various modulation schemes are investigated for the Gigabit per second (Gbps) wireless infrared (IR) line-of-sight (LOS) communication. The power and bandwidth efficiency are compared while considering the impact of shot noise and  $f^2$  noise as well as distortions caused by a noise rejection filter and a high-pass filter (HPF) at the receiver. Furthermore, the wireless IR transmission can be seriously deteriorated by the so called “transient baseline wander”, which is caused by the inherent high-pass characteristic of the receiver. This signal distortion induced by such an impairment can be mitigated by using a line code such as the “IBM 8B10B code”.

**Index Terms**— optical wireless transmission, modulation, OOK, line coding, 8B10B, noise, photodiode

## 1. INTRODUCTION

Home networks at speeds of several Gbps are a pivotal technology for realizing the European Union’s (EU’s) vision of the future Internet. As a part of the EU Seventh Framework R&D programme (FP7), the OMEGA project [www.ict-omega.eu] investigates and optimizes the three main technologies for home access, i.e., radio frequency, wireless optical and power line.

This paper is focused on Gbps wireless IR LOS communication [1], which requires intensity modulation and direct detection [2]. In order to ensure Gbps transmission over several meters, an appropriate modulation scheme has to be selected carefully.

The power efficiency of various modulation schemes is usually compared by assuming additive white Gaussian noise, where the background light induced shot noise is considered as the strongest source of noise. While this noise model holds for moderate data rates of several tens of Mbps, it is not valid for 1 Gbps and beyond, if PIN receivers, which are affected by strong  $f^2$  noise, are used. This contribution shows that a modulation scheme, which may perform well in white noise, is not necessarily a good choice when  $f^2$  noise dominates.

Popular modulation schemes are on-off keying (OOK) and pulse-position modulation (PPM) [3].

In this paper, OOK based on non-return-to-zero rectangular pulses (NRZ-OOK) is chosen as the reference modulation scheme. This scheme is compared to return-to-zero OOK (RZ-OOK), 4-PPM, and various subcarrier modulations (like phase-shift keying (PSK) and quadrature amplitude modulation (QAM)) in terms of the required bandwidth and power. These investigations show the feasibility of NRZ-OOK for the Gbps IR OMEGA demonstrator.

The robustness to high-pass filtering is also considered. While subcarrier modulation and 4-PPM do not include low frequency spectral components, it is not the case for OOK. For this reason, OOK has to be combined with a line code. The “IBM 8B10B code” [4] is a very favourable candidate.

This paper is organized as follows. Section 2 describes the simulation system. Section 3 gives an analytical overview about several selected modulation schemes and Section 4 explains the reason for integrating the “IBM 8B10B code”. This paper ends in Section 5 and 6 with simulation results and a summary.

## 2. GBPS WIRELESS IR SYSTEM

The block diagram of the Gbps wireless IR system is shown in Fig. 1. The transmitter consists of an intensity modulator which drives a laser diode, and optionally of a line encoder. The optical signal passes through a LOS channel, which is assumed to be ideal and characterized by the impulse response  $h_c(t) = \delta(t)$ .

At the receiver, the incoming optical signal is converted into an electrical signal by a PIN photodiode (PIN-PD) or an Avalanche photodiode (APD). This electrical signal comprises of the transmitted signal and the ambient light induced shot noise that is essentially white Gaussian distributed and independent of the desired signal.

Although the transfer function of the preamplifier at the receiver frontend is assumed to be ideal with  $|H_{\text{preamp}}(f)| = 1$ , its induced noise is considered. This

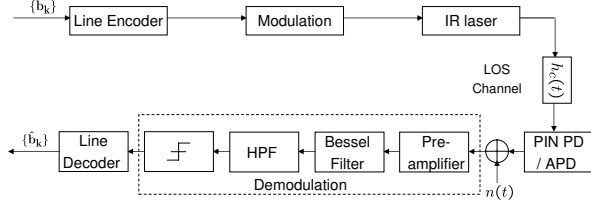


**Fig. 1.** Block diagram of the Gbps wireless IR system

additional noise, which is referred to the receiver input, consists of thermal noise with constant power spectral density (PSD) and  $f^2$  noise with PSD increasing with the square of the frequency [5]. It should be noted that the noise variance of  $f^2$  noise depends on  $R_b^3$ . That means, changing the data rate  $R_b$  from 100 Mbps to 1 Gbps will result in an increased power of the  $f^2$  noise by a factor of 1000. Because of that  $f^2$  noise mainly degrades the receiver sensitivity for indoor Gbps wireless IR transmission.

A 5th-order Bessel low-pass filter is then applied for noise rejection with its cut-off frequency  $f_{3dB} = B_{req}/2$ . The HPF, which is modeled as a first order RC filter, is used for mitigating the fluorescent light induced periodic interference. In this paper, the cut-on frequency of this HPF is defined as  $f_c = 0.005 \cdot B_{req}$ . It provides a good tradeoff between the vertical eye-opening, the reduction of fluorescent light harmonics and the required small settling time of around 8 bytes at a data rate of 1 Gbps. But, it could result in the transient baseline wander effect. After HD, the demodulated signal is decoded to retrieve the transmitted data.

A key point with respect to the high-speed wireless IR system design is the choice of the wavelength. The wavelength range at around 850 nm was found to be best suited, since silicon photodiodes are available at low costs and offer a good compromise between the transit time, the capacitance and the responsivity.

Furthermore, with respect to the receiver design, silicon PIN-PDs and APDs are to be investigated separately for different modulation schemes. A small photodiode capacitance is definitely desirable for both photodiodes due to its square proportionality to the variance of the  $f^2$  noise [6]. The capacitance per unit area of about 5 pF/mm<sup>2</sup> can be viewed as an excellent choice for a well designed silicon photodiode with a responsivity of  $R_\lambda = 0.5$  A/W and a transit time of around 0.5 ns. Based on those considerations, various modulation schemes are to be exploited in the next section.

### 3. MODULATION SCHEMES

In this section, NRZ-OOK will be used as a benchmark to compare the bandwidth and power efficiencies of various simple and predominant binary modulation schemes. While disturbances due the noise rejection

filter as well as additive noise components at the receiver are taken into account within this section, the HPF and the line code are not included for simplicity.

#### 3.1. NRZ-OOK

For any binary modulation scheme, the bit error rate (BER)  $p_b$  can be expressed as a function of the electrical signal-to-noise ratio (SNR)  $\varrho$  [7]

$$p_b = \frac{1}{2} \operatorname{erfc} \sqrt{\frac{\varrho}{2}} \quad \text{with} \quad \varrho = \frac{(d_{EO}/2)^2}{\sigma_n^2}, \quad (1)$$

where  $d_{EO}$  is the maximum vertical eye-opening supposing that the filters cause no signal distortion.  $\sigma_n^2$  denotes the noise variance. Assuming NRZ-OOK rectangular pulses with its peak optical signal power  $\hat{P}_{rx}$  at the receiver and thus its average optical power  $P_{rx} = \hat{P}_{rx}/2$ , the ideal vertical eye-opening is

$$d_{EO} = 2P_{rx}R_\lambda M.$$

$M$  is the multiplication factor of the photodiode (APD-gain), with  $M = 1$  for PIN-PDs and  $M$  ranges from 1 to 100 for typical APDs.

Furthermore, the vertical eye-opening penalty  $K_{EOP} = d/d_{EO} \leq 1$  is defined to describe the loss of the vertical eye-opening  $d$  caused by a filter with a certain bandwidth. In general, the required bandwidth for a modulation scheme is defined by the first zero crossing of the PSD of its base function. For NRZ-OOK, the required filter bandwidth is  $B_{req} = R_b$ , if no line code is considered. Thus the cut-off frequency of the 5th-order Bessel low-pass filter at the receiver is assumed to  $f_{3dB} = R_b/2$ . Then Eq. (1) becomes

$$p_b = \frac{1}{2} \operatorname{erfc} \left( \frac{K_{EOP} \cdot P_{rx} R_\lambda M}{\sqrt{2} \cdot \sqrt{\sigma_n^2}} \right)$$

and the required average optical receiving power is

$$P_{rx} = \frac{\sqrt{2} \cdot \sqrt{\sigma_n^2}}{K_{EOP} \cdot R_\lambda M} \cdot \operatorname{erfc}^{-1}(2p_b).$$

For a BJT-based preamplifier, the noise variance  $\sigma_n^2$  after the HPF and the Bessel filter is given as [7]

$$\begin{aligned} \sigma_n^2 &= \int_0^\infty 2\Phi_{nn}(f) |H_{rx}(f)|^2 df \\ &= \sigma_{n,N_0}^2 + \sigma_{n,N_2}^2 \\ &= \underbrace{\left( 2qP_{bg}R_\lambda M^2 F(M) + 2qI_b + \frac{4k_B T}{R_L} \right)}_{N_0} I_2 R_b + \\ &\quad \underbrace{\left( \frac{2qI_c (2\pi C_{tot})^2}{S^2} + 4k_B T (R_s + R_{bb}) (2\pi C_D)^2 \right)}_{N_2} I_3 R_b^3. \end{aligned} \quad (2)$$

- $N_0$  represents the one-side PSD of the white noise, of which the first item gives the background light induced shot noise and the rest are due to the preamplifier at the receiver frontend.  $N_2$  is the one-side PSD of the  $f^2$  noise caused by the preamplifier.

- $P_{bg}$  is the background light power. The term

$$F(M) = k_A M + (1 - k_A)(2 - 1/M)$$

is the excess noise factor, where  $k_A$  is the effective ionization ratio typically varying between 0.02 and 0.05 for silicon photodiodes. Here a factor of 0.02 is assumed.

- $q$  electronic charge;  $k_B$  Boltzmann constant;  $T$  absolute temperature

- $I_b$  is the base current of the BJT at the first stage of the preamplifier and  $I_c = \beta I_b$  is the collector current which contributes to the  $f^2$  noise with current gain  $\beta$ . The transconductance of the transistor is  $S = \frac{qI_c}{k_B T}$ .

- $C_D$  is the photodiode capacitance and  $C_{tot} \approx C_D$  is the total capacitance at the first stage of the preamplifier.  $R_L$  is the load resistor and  $R_s + R_{bb}$  is the sum of the photodiode series resistance and the BJT-spreading resistance.

- 

$$I_2 = \int_0^\infty |H_{rx}(f')|^2 df',$$

$$I_3 = \int_0^\infty f'^2 |H_{rx}(f')|^2 df'$$

are the Personick-integrals for the white noise and the  $f^2$  noise respectively, where  $f' = f/R_b$  and  $|H_{rx}(f)|$  denoting the transfer function of the combination of the preamplifier, the Bessel low-pass and the HPF. Considering a 5th-order Bessel filter with  $f_{3dB} = R_b/2$ , these parameters are given as  $I_2 = 0.52$  and  $I_3 = 0.0843$ .

### 3.2. RZ-OOK

A return-to-zero rectangular pulse with a duty cycle of 0.5 is to be investigated on the basis of the same average receiving power  $P_{rx}$  as for NRZ-OOK. The optical peak power is  $\hat{P}_{rx} = 4P_{rx}$  and the ideal vertical eye-opening is

$$d_{EO} = 4P_{rx} R_\lambda M.$$

The required average receiving power for RZ-OOK is

$$P_{rx} = \frac{\sqrt{\sigma_n^2}}{\sqrt{2} \cdot K_{EOP} \cdot R_\lambda M} \cdot \operatorname{erfc}^{-1}(2p_b).$$

Deviant of the constraint  $f_{3dB} = B_{req}/2$ , for RZ-OOK the cut-off frequency of the Bessel filter is assumed to  $f_{3dB} = R_b/2$  for further studies to reduce the noise variance while maintaining the form of the RZ pulses.

### 3.3. OOK based on a Subcarrier

The modulation, OOK based on a subcarrier (OOK Sub), is similar to NRZ-OOK by using a cosine pulse instead of a rectangular one. Power “on” is expressed by  $s_1(t) = P_{rx} \left(1 - \cos\left(2\pi \frac{t}{T_b}\right)\right)$  constrained in  $[0, T_b]$  while “off” by  $s_2(t) = 0$ . The optical peak power is  $\hat{P}_{rx} = 4P_{rx}$  and the ideal vertical eye-opening is

$$d_{EO} = 4P_{rx} R_\lambda M.$$

The required average receiving power for OOK Sub is

$$P_{rx} = \frac{\sqrt{\sigma_n^2}}{\sqrt{2} \cdot K_{EOP} \cdot R_\lambda M} \cdot \operatorname{erfc}^{-1}(2p_b).$$

### 3.4. 4-PPM

In 4-PPM, each symbol interval of duration  $T_s = 2T_b$  is partitioned into  $L = 4$  chips of duration  $T_c = T_s/4 = T_b/2$ . With the assumption of the same average receive power  $P_{rx}$  as for NRZ-OOK, the optical peak power of the rectangular pulses is  $\hat{P}_{rx} = 4P_{rx}$  and the ideal vertical eye-opening is

$$d_{EO} = 4P_{rx} R_\lambda M.$$

According to [3], the symbol error rate for HD is approximated as

$$p_{s,HD} \approx \frac{L}{2} \cdot \operatorname{erfc} \left( \sqrt{\frac{\rho}{2}} \right)$$

and the BER is given as

$$p_{b,HD} = \frac{L}{2(L-1)} p_{s,HD}$$

$$= \frac{4}{3} \operatorname{erfc} \left( \frac{\sqrt{2} \cdot K_{EOP} \cdot P_{rx} R_\lambda M}{\sqrt{\sigma_n^2}} \right).$$

It has to be noted that the noise variance is not the same as before. The Personick-integrals are  $I_{2,PPM} = 2I_2$  and  $I_{3,PPM} = 8I_3$  because a Bessel filter with a cut-off frequency  $f_{3dB} = R_b$  is applied for 4-PPM due to its doubled bandwidth  $B_{req} = 1/T_c = 2R_b$ . Furthermore, in this case, the photodiode has to be as twice as fast. Considering a factor of  $\sqrt{2}$  caused by the HD constraint, the required average receiving power for 4-PPM is

$$P_{rx} = \frac{\sqrt{\sigma_n^2}}{K_{EOP} \cdot R_\lambda M} \cdot \operatorname{erfc}^{-1} \left( \frac{3}{4} p_b \right).$$

Even if 4-PPM is regarded as coded OOK with [1000], [0100], [0010], [0001], this assumption is valid due to the inherent reduction of the number of transmitted ones.

### 3.5. BPSK

BPSK uses either  $s_1(t) = P_{\text{rx}} \left(1 - \cos\left(2\pi \frac{t}{T_b}\right)\right)$  or  $s_2(t) = P_{\text{rx}} \left(1 + \cos\left(2\pi \frac{t}{T_b}\right)\right)$  constrained in  $[0, T_b]$  for transmitting the signal “on” and “off” separately. The ideal vertical eye-opening after down conversion is

$$d_{\text{EO}} = \sqrt{2} P_{\text{rx}} R_{\lambda} M.$$

Due to the required down conversion from the subcarrier at the receiver, simulated as a multiplication with  $m_1(t) = \sqrt{2} \cos\left(2\pi \frac{t}{T_s}\right)$ , the noise variance has to be recalculated as (cf. Appendix for more details)

$$\begin{aligned} \sigma_n^2 &= \int_0^{\infty} (N_0 + N_2 f^2) * \frac{1}{2} [\delta(f - R_b) + \delta(f + R_b)] \\ &= N_0 I_2 R_b + N_2 (I_2 + I_3) R_b^3. \end{aligned} \quad (3)$$

The required average receiving power for BPSK is

$$P_{\text{rx}} = \frac{2 \cdot \sqrt{\sigma_n^2}}{K_{\text{EOP}} \cdot R_{\lambda} M} \cdot \text{erfc}^{-1}(2p_b).$$

### 3.6. 4-QAM

4-QAM provides the 4 different signals

$$s_i(t) = P_{\text{rx}} \pm \frac{P_{\text{rx}}}{\sqrt{2}} \cos\left(2\pi \frac{t}{T_s}\right) \pm \frac{P_{\text{rx}}}{\sqrt{2}} \sin\left(2\pi \frac{t}{T_s}\right)$$

constrained in  $[0, T_s] \forall i = 1, 2, 3, 4$  with the symbol time  $T_s = 2T_b$  to modulate two different bits simultaneously. The ideal vertical eye-opening after down conversion, separately for the inphase and quadrature path, is

$$d_{\text{EO}} = \sqrt{2} P_{\text{rx}} R_{\lambda} M.$$

The required average receiving power for 4-QAM is

$$P_{\text{rx}} = \frac{2 \cdot \sqrt{\sigma_n^2}}{K_{\text{EOP}} \cdot R_{\lambda} M} \cdot \text{erfc}^{-1}(2p_b).$$

At the receiver, which is shown in Fig. 2, the high-pass filtered signal with a cut-on frequency of

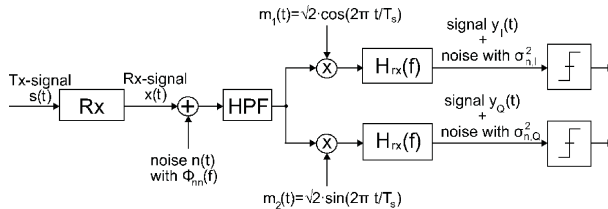


**Fig. 2.** Receiver design for 4-QAM. (The cut-on frequency of the HPF is  $f_c = 0.0075 \cdot R_b$  and the transfer function of the noise rejection filter  $H_{\text{rx}}(f)$  is assumed as a root raised cosine (RRC) function with a roll-off factor of 1.)

$f_c = 0.0075 \cdot R_b$  has to be down converted before it is fed into a suitable noise rejection filter. This down conversion is performed by a multiplication with  $m_1(t) = \sqrt{2} \cos\left(2\pi \frac{t}{T_s}\right)$  and  $m_2(t) = \sqrt{2} \sin\left(2\pi \frac{t}{T_s}\right)$  to provide the inphase and the quadrature path respectively. For both paths, the same noise variance is obtained as in Eq. (3) due to the down conversion (cf. Appendix).

The Personick-integrals are determined as  $I_2 = 0.25$  and  $I_3 = 0.0082$  because of the according symbol rate for 4-QAM  $R_s = R_b/2$  and the usage of a root raised cosine (RRC) filter for noise rejection ( $H_{\text{rx}}(f)$ ) with a roll-off factor of 1. This RRC filter is applied instead of the 5th-order Bessel low-pass filter which violates the orthogonality of the inphase and the quadrature path.

Besides, at the transmitter, the signal has to be adopted additionally to this RRC pulse form (displayed in Fig. 3) to prepare the demodulation with the proposed filter.

The analytical comparison between the abovementioned modulation schemes is shown in Table 1. BPSK is not a good candidate because of its high loss caused by the Bessel filter and the noise amplification due to the use of the subcarrier. Because of the doubled bandwidth of 4-PPM which increases the  $f^2$  noise and due to the requirement of faster photodiodes, 4-PPM is not a real alternative to NRZ-OOK. Although 4-QAM depicts very good results in Table 1, it is not chosen as a suitable modulation method due to the complexity of the transmitter and the receiver design and the accompanying increase of the  $f^2$  noise shown in Eq. (3).

RZ-OOK and OOK Sub are possible alternatives to NRZ-OOK in terms of power efficiency, bandwidth efficiency or reasonable leakage. However, OOK can be considered as a good choice for Gbps transmission and NRZ-OOK is chosen for the Gbps IR OMEGA demonstrator because of its extreme implementation simplicity for the laser diode as well as for the receiver.

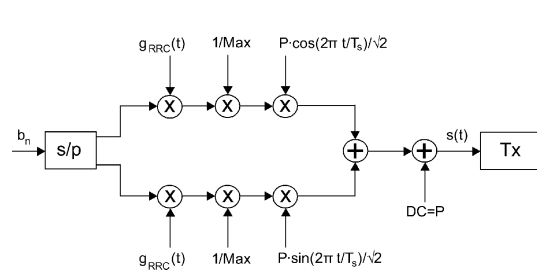


**Fig. 3.** RRC pulse forming at the transmitter

Modulation Method	Required Bandwidth $B_{\text{req}}$	$d_{\text{EO}}/(R_{\lambda}M)$	Bessel Filter Cut-Off Frequency $f_{3\text{dB}}$	$K_{\text{EOP}}$ due to the Noise Rejection Filter
NRZ-OOK	$R_b$	$2P$	$0.5R_b$	0.90
RZ-OOK	$2R_b$	$4P$	$0.5R_b$	0.63
			$R_b$	0.95
OOK Sub	$0.7R_b$	$4P$	$0.5R_b$	0.60
4-PPM	$2R_b$	$4P$	$R_b$	0.90
BPSK	$R_b$	$\sqrt{2}P$	$0.5R_b$	0.84
4-QAM	$0.5R_b$	$\sqrt{2}P$	-	0.91

**Table 1.** Comparison of different modulation schemes

#### 4. LINE CODING

In this section, the desired line coding suitable for Gbps IR transmission is to be demonstrated based on NRZ-OOK. According to [8], the following properties are further considered in selecting a proper line code for high-speed IR links:

- **Code rate**  $R_c = m/n$ : is determined as the ratio between the number of input bits  $m$  and the number of coded output bits  $n$ , whereas high code rates are desired.
- **DC-balance**: is preferable because it ensures the optimum decision threshold at zero with respect to the high-pass filtered signal. DC-balance means that the disparity (DP) of all acceptable code words, defined as the difference between the count of ones and zeros within a code word, is zero. The running disparity (RD) characterizes the sum of the DP of all code words from the beginning of a transmission until the current transmitted code word. A constant and small RD is desired because it provides robustness towards the transient baseline wander caused by the receive-site HPF.
- **Maximum run-length**  $r_{\text{max}}$ : is defined as the maximum number of consecutive ones or zeros within the coded data stream that needs to be limited to provide regular clock information.
- **Short time average variation**  $\sigma_N$ : The HPF at the receiver is assumed to be a first order RC-filter with the step response

$$g(t) = \delta(t) - \frac{1}{T} \exp\left(-\frac{t}{T}\right) \quad \text{for } t \geq 0,$$

which shows that it basically removes the short time average from the signal. The transient baseline wander effect can still be estimated roughly assuming constant weighting factors within the integration interval. With  $c_n \in \{0, 1\}$  being code

bits at the line encoder output,

$$\mu_N[n] = \frac{1}{N} \sum_{k=n}^{n+N-1} c_k, \quad n \in \mathbb{N}$$

is defined as the short time average over  $N$  bits. The relative vertical eye-opening at the receiver can be estimated as

$$(1 - \mu_{N,\text{max}}) - (0 - \mu_{N,\text{min}}) = \frac{1 - (\mu_{N,\text{max}} - \mu_{N,\text{min}})}{\sigma_N},$$

with

$$\mu_{N,\text{max}} = \max_{\forall n} \mu_N[n]$$

and

$$\mu_{N,\text{min}} = \min_{\forall n} \mu_N[n]$$

denoting the maximum and minimum short time average over  $N$  bits respectively.  $\sigma_N$  is the maximum variation of the short time average and a direct measure of the loss with respect to the vertical eye-opening which is desired to be as low as possible. For example, 4-PPM can also be considered as line coded OOK transmission with  $R_c = 1/2$ .  $\sigma_{10} = 1/5$  and  $\sigma_{20} = 1/10$  are obtained for 4-PPM, showing that the transient baseline wander effect decreases with an increasing integration interval [8].

Fig. 4 gives the DP variation of various theoretical  $mBnB$  codes with respect to the code rate. The relationship between the number of input and output bits is determined by the count  $K$  of possible code words for a given DP:

$$K_i = \sum_{j=0}^i \binom{n}{n/2 - \text{DP}_j/2}$$

with

$$\text{DP}_i \in \{\text{DP}_{i-1}, \pm 2i\} \quad \text{for } i \geq 1 \quad \text{and } \text{DP}_0 = 0$$

resulting in

$$m = \lfloor \log_2(K) \rfloor.$$

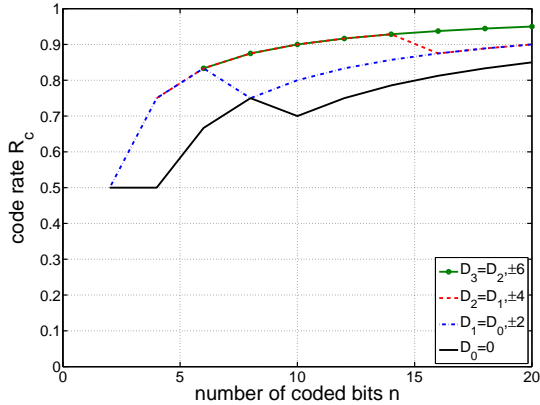


**Fig. 4.** Disparity variation vs. code rate

Since the  $f^2$  noise is the main obstacle in limiting the receiver sensitivity, it implies that low redundancy is a primary design issue in choosing a proper line code due to the fact that the variance of the  $f^2$  noise also depends on the third power of the data rate  $R_b^3$  (cf. Eq. (2)). It clearly shows that the 8B10B code provides a very good DC-balance while maintaining a higher code rate. Although the 5B6B code displays the same DP variation at a slightly higher code rate of  $R_c = 0.833$ , the natural affinity with the data packet units at the MAC layer and the byte rate clock make the 8B10B code even more preferred.

From this analysis, the “IBM 8B10B code” is proposed for the Gbps IR OMEGA demonstrator, which has already been used in many systems including the Gigabit Ethernet. The main feature of this code is that it is a concatenation of a 5B6B code and a 3B4B code. Encoding and decoding are performed independently for each 6B or 4B subblock by using a look-up table. Moreover, all 6B and 4B subblocks individually, and the complete 10-bit code word hold a DP of either 0 or  $\pm 2$ , which ensures quite a small transient baseline wander as expressed using short time average  $\sigma_{20} = 0.3$  because of the achieved DC-balance over several code words. To create such a DC-balanced code during the transmission, the rule of RD has to be fulfilled for every 4B and 6B subblock. That means, if the current RD is positive, a code word with a negative DP or a DP of zero is selected after initialising  $RD = -1$  and vice versa. Besides, the maximum run-length of this code is limited to 4 which ensures the required clock recovery at the receiver. A more detailed description of the “IBM 8B10B code” can be found in [4] and [8].

## 5. SIMULATION RESULTS

The first step of this analysis contains the verification of the following hypotheses with respect to NRZ-OOK as the modulation benchmark:

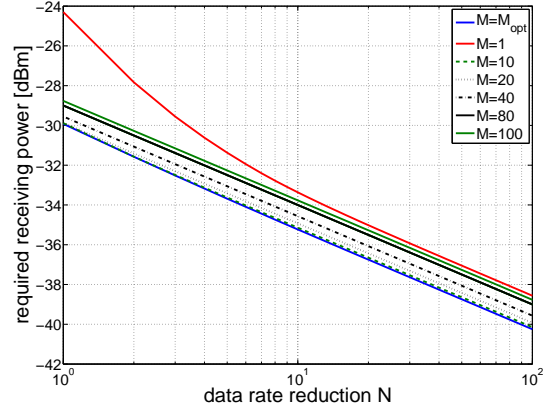


**Fig. 5.** Required optical receiving power for NRZ-OOK depending on the data rate  $R_b/N$  with  $R_b = 1.25$  Gbps for different values of the APD-gain  $M$ . (Including the “IBM 8B10B code” and the according penalty due to the Bessel filter and the HPF.)

- The part of white noise mainly determines the required optical receiving power for APDs due to its optimal value for the APD-gain  $M$ , whereas for PIN-PDs with  $M = 1$  the  $f^2$  noise dominates the required optical receiving power due to the proportionality to  $R_b^3$  (cf. Eq. (2)), especially at higher data rates.
- The amount of background light  $L_{bg}$  is one of the most important noise parameters, especially for APDs.
- Ideal APD receivers with an optimal APD-gain can be approximated by APDs with a fixed value of the APD-gain.

At the second step, different modulation schemes are investigated with respect to the required optical receiving power.

Assuming a data rate on the line for NRZ-OOK of  $R_b = 1.25$  Gbps due to the required “IBM 8B10B code”, a BER of  $p_b = 10^{-9}$ , an average radiance of the background light of  $L_{bg} = 2 \mu\text{W}/(\text{mm}^2 \cdot \text{sr})$  and an area of the photodiode of  $1 \text{ mm}^2$ , Fig. 5 depicts that the required optical receiving power increases with the data rate. This power decrease is linear for APDs with an APD-gain of  $M > 1$ . But for PIN-PDs, where  $M = 1$ , this decrease is more exponential for small values of the data rate reduction  $N$ , due to the proportionality of the variance to the 3rd power of the data rate (cf. Eq. (2)). At first, it can be assumed that there will be a power gain of a factor of  $\sqrt{N}$  for APDs according to the white noise variance components and for PIN-PDs a gain of a factor of  $\sqrt{N^3}$  according to the  $f^2$  noise variance components while reducing the data rate by  $N$ . The simulation of Fig. 5 shows that the power gain



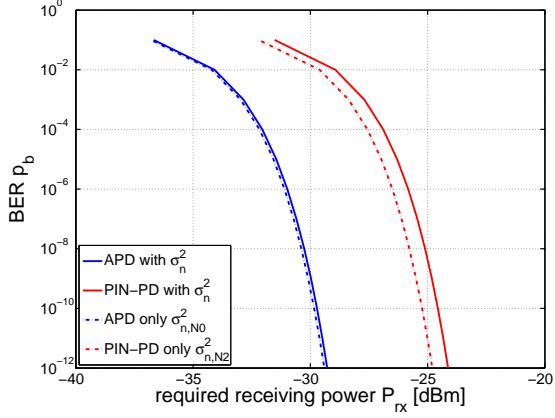


**Fig. 6.** Required optical receiving power for NRZ-OOK for APDs and PIN-PDs considering the total noise variance  $\sigma_n^2$  of Eq. (2) or only a part of it ( $\sigma_{n,N_0}^2$  or  $\sigma_{n,N_2}^2$ ). The “IBM 8B10B code” and the penalty due to the Bessel and the HPF are included.

for ideal APDs is a little bit higher than predicted because not only the white noise, also other noise components will be reduced while reducing the data rate. On the contrary, the power gain of PIN-PDs is smaller than predicted, because the white noise part still dominates for PIN-PDs at data rates lower than 100 Mbps and can not be neglected anymore.

Fig. 6 shows for NRZ-OOK the required optical receiving power versus the BER for APDs and PIN-PDs considering either the total noise variance  $\sigma_n^2$  of Eq. (2) or only a part of it,  $\sigma_{n,N_0}^2$  or  $\sigma_{n,N_2}^2$ . This simulation verifies the applicable approximation of the required optical receiving power for APDs by considering only white noise components and for PIN-PDs by only considering  $f^2$  noise components at data rates of around 1 Gbps. Only for PIN-PDs there is a bigger inaccuracy due to the additional part of the white noise for PIN-PDs predominantly caused by the assumed high average background light.

The analysis of the influence of the background light at a data rate of 1.25 Gbps depicts that the required optical receiving power is almost independent of the background light for PIN-PDs. But for APDs, Fig. 7 represents a strong increase of the required optical receiving power when increasing the background light.

Furthermore, Fig. 5 and Fig. 7 verify that a constant APD-gain of  $M \in [10, 40]$  will be a good choice to approximate the performance of an ideal APD-gain, especially by assuming an average background light in the range of  $L_{bg} = 2 \mu\text{W}/(\text{mm}^2 \cdot \text{sr})$ . A radiance of the background light of about  $L_{bg} = 0.002 \mu\text{W}/(\text{mm}^2 \cdot \text{sr})$  yields about 20 nA current which is arranged in the dimension of the dark current of the photodiode and does not represent the standard case. Besides, all these simulations depend on the area of the photodiode, too. In

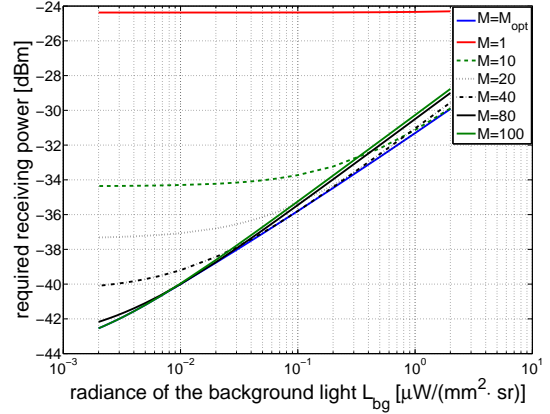


**Fig. 7.** Required optical receiving power for NRZ-OOK depending on the background light  $L_{bg}$  for different values of the APD-gain  $M$ . (Including the “IBM 8B10B code” and the according penalty due to the Bessel and the HPF.)

general, the required optical receiving power increases with the photodiode area.

Fig. 8 shows the results for the required optical receiving power for all the abovementioned modulation methods under the usage of a PIN-PD and Fig. 9 depicts the results under the usage of an ideal APD with its optimal APD-gain. In both cases, only RZ-OOK and OOK Sub represent a better performance than the reference NRZ-OOK with a gain of approximately 1.5 dB, although a line code is included for them (e.g. the “IBM 8B10B code” which increases the data rate up to  $R_b = 1.25$  Gbps and thus the critical frequencies of the filters at the receiver to  $f_{3dB} = 650$  MHz and  $f_c = 6.5$  MHz and decreases the loss due to the transient baseline wander effect, too). 4-PPM, BPSK and 4-QAM do not need a line code because 4-PPM can still be regarded as coded OOK, while BPSK and 4-QAM always generate alternating pulses within one symbol interval which ensure the clock recovery. Although 4-QAM shows a better performance as NRZ-OOK for APDs, this method is excluded because of the much higher complexity at both the transmitter and the receiver (cf. Section 3).

All in all, due to the simplicity of NRZ-OOK which provides only two different amplitude levels, it is chosen as the modulation method for the Gbps IR OMEGA demonstrator. Moreover, under this consideration, the according transmit-site laser driver is easier to build and more power efficient than linear drivers which are necessary for subcarrier modulation (e.g. OOK Sub and 4-QAM) with its changing amplitude values within one symbol. Furthermore, if the “IBM 8B10B code” is included, which offers almost DC-balance, the decision threshold for NRZ-OOK has not to be derived from the

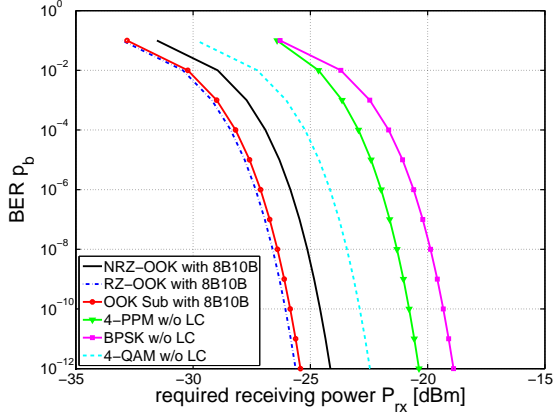


**Fig. 8.** Comparison of different modulation schemes based on PIN-PDs where line coding is included if necessary. (The loss due to the 5th-order Bessel low-pass and the first order RC HPF is always included.)

received signal which is required for RZ-OOK or 4-PPM. In the case of DC-balance, the decision threshold is equal to zero because of the HPF at the receiver.

## 6. CONCLUSION

In this paper, NRZ-OOK and the “IBM 8B10B code” is proposed to be practically applied in the Gbps wireless IR transmission system considering the effect of a 5th-order Bessel low-pass filter for noise rejection, a HPF in order to mitigate the fluorescent light interference as well as the noise components of the preamplifier at the receiver. The simulation results show the comparison between various modulation schemes in terms of power efficiency based on PIN-PDs and APDs. OOK based modulation schemes offer a good compromise between power and bandwidth efficiency, whereas APDs provide a 5 dB gain compared to PIN-PDs. Moreover, its implementation simplicity makes NRZ-OOK preferred for the Gbps IR OMEGA demonstrator.

The baseline wander induced by the use of the HPF can be effectively mitigated using the proposed “IBM 8B10B code”, which also ensures efficient clock recovery due to sufficient transitions available. To conclude, a reasonable link budget can be observed by applying NRZ-OOK in concatenation with the “IBM 8B10B code” in the Gbps wireless IR LOS communication.

## 7. REFERENCES

[1] K.-D. Langer, O. Bouchet, D. C. O’Brien, and M. Wolf, “Optical Wireless Communications for Broadband Access in Home Area Networks,” *International Conference on Transparent Optical Networks*, vol. 4, pp. 149–154, 2008.

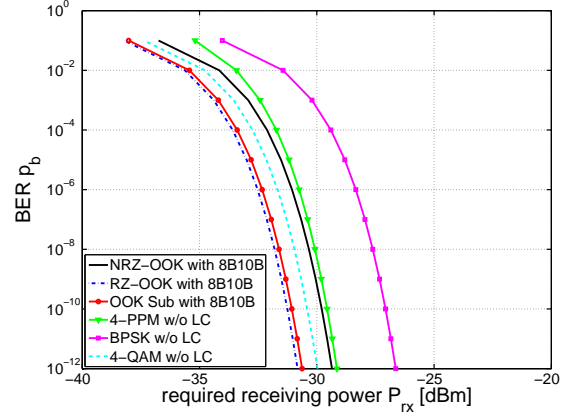


**Fig. 9.** Comparison of different modulation schemes based on ideal APDs where line coding is included if necessary. (The loss due to the 5th-order Bessel low-pass and the first order RC HPF is always included.)

[2] M. Wolf and M. Haardt, “Coding Limits for Short Range Wireless Infrared Transmission,” in *16th Annual IEEE International Symposium on Personal Indoor Radio Communications (PIMRC’05)*, vol. 2, 2005, pp. 1065–1070.

[3] J. R. Barry, *Wireless Infrared Communications*, 1. edition, Dordrecht, The Netherlands: Kluwer Academic Publishers Group, 1994.

[4] A. X. Widmer and P. A. Franaszek, “A DC-Balanced, Partitioned-block, 8B/10B Transmission Code,” *IBM Journal of research and development*, vol. 27, Sept. 1983.

[5] T. v. Muoi, “Receiver Design for High-Speed Optical-Fiber Systems,” *Journal of Lightwave Technology*, vol. LT-2, no. 3, pp. 243–267, 1984.

[6] S. D. Personick, “Receiver Design for Optical Fiber Systems,” *Proc. of the IEEE*, vol. 65, pp. 1670–1678, 1977.

[7] J. G. Proakis, *Digital Communications*, 3. edition, New York: McGraw-Hill, 1995.

[8] J. Li, M. Wolf, and M. Haardt, “Investigation of the Baseline Wander Effect on Gbps Wireless Infrared System Employing 8B10B Coding,” in *International Conference on Telecommunications*, 2009.

## 8. APPENDIX

The influence on the noise due to the subcarriers can be investigated by the convolution of the PSD of the white or the  $f^2$  noise with the PSD of the subcarriers where

$R_s$  represents the symbol rate.

The PSD of white and  $f^2$  noise is given as:

$$\Phi_{N_0, N_0}(f) = \frac{N_0}{2} \quad \text{and} \quad \Phi_{N_2, N_2}(f) = \frac{N_2}{2} \cdot f^2$$

Definition of the cosine subcarrier  $m_1(t)$  and the sine subcarrier  $m_2(t)$  in the frequency domain:

$$M_1(f) = \frac{\sqrt{2}}{2} \cdot [\delta(f - R_s) + \delta(f + R_s)]$$

and

$$M_2(f) = j \frac{\sqrt{2}}{2} \cdot [\delta(f + R_s) - \delta(f - R_s)]$$

Calculated PSD of the cosine and the sine subcarrier:

$$\begin{aligned} \Phi_{M_1, M_1}(f) &= |M_1(f)|^2 = \Phi_{M_2, M_2}(f) = |M_2(f)|^2 \\ &= \frac{1}{2} \cdot [\delta(f - R_s) + \delta(f + R_s)] \end{aligned}$$

Results of the convolution for white noise:

$$\begin{aligned} \Phi_{N_0, N_0}(f) * \Phi_{M_1, M_1}(f) &= \Phi_{N_0, N_0}(f) * \Phi_{M_2, M_2}(f) \\ &= \frac{N_0}{2} \end{aligned}$$

Results of the convolution for  $f^2$  noise:

$$\begin{aligned} \Phi_{N_2, N_2}(f) * \Phi_{M_1, M_1}(f) &= \Phi_{N_2, N_2}(f) * \Phi_{M_2, M_2}(f) \\ &= \frac{N_2}{2} \cdot f^2 * \frac{1}{2} \cdot [\delta(f - R_s) + \delta(f + R_s)] \\ &= \frac{N_2}{4} (f - R_s)^2 + \frac{N_2}{4} (f + R_s)^2 \\ &= \frac{N_2}{4} \cdot [f^2 - 2R_s f + R_s^2 + f^2 + 2R_s f + R_s^2] \\ &= \frac{N_2}{2} \cdot f^2 + \frac{N_2}{2} \cdot R_s^2 \end{aligned}$$